*lubricants*

MDPI

*Article*

# Static and Dynamic Friction of Pure and Friction-Modified PA6 Polymers in Contact with Steel Surfaces: Influence of Surface Roughness and Environmental Conditions

**Joel Voyer *, Stefan Klien, Igor Velkavrh, Florian Ausserer and Alexander Diem**

V-Research GmbH, Stadtstrasse 33, 6850 Dornbirn, Austria; stefan.klien@v-research.at (S.K.); igor.velkavrh@v-research.at (I.V.); florian.ausserer@v-research.at (F.A.); alexander.diem@v-research.at (A.D.)

* Correspondence: joel.voyer@v-research.at; Tel.: +43-5572-394-159-36

Received: 30 November 2018; Accepted: 13 February 2019; Published: 16 February 2019


**Abstract:** In the present study, PA6 polymers with and without solid lubricant inclusions were investigated against S1100QL steel surfaces that had different surface roughness values—a very high surface roughness ($R_z \approx 40$ µm) and a low surface roughness ($R_z \approx 5$ µm). Static and dynamic friction coefficients were analysed under a series of nominal contact pressures (2.5 to 40 N/mm$^2$) considering the influences of polymer water saturation, temperature, counter-body surface roughness and lubrication. Mechanisms for the observed influences of the respective parameters are provided and are interpreted from the view of the adhesive and deformative contributions to the friction force.

**Keywords:** polymer tribology; sliding contacts; surface roughness; adhesion; deformation

## 1. Introduction

Over the past years, polymers have gained a tremendous interest among the scientific and industrial communities as an alternative to metals in a variety of engineering applications, mainly due to their relatively low cost, ease of processing even complex component geometries through a variety of production processes, chemical inertness, the ability to be used in dry friction and recyclability [1–4].

Additionally to pure polymers, developments of new polymer composites based on commercially available conventional polymers may result in a new series of materials that have enhanced thermal, mechanical and tribological properties [1,5–7].

The main mechanisms determining friction forces (and subsequently friction coefficients) for polymers are adhesion and deformation, as schematically shown in Figure 1. Depending on the polymer and on its adhesive and mechanical properties, the friction force has a strong dependency on surface roughness and normal load. For a high number of polymers, adhesive friction is dominant at low loads but at high loads, deformative friction becomes more important. For polymers with a high load bearing capability like PA6, the coefficient of friction (COF) mostly decreases with increasing load because of a change in the dominant friction mechanism.

In some applications, optimized smooth surfaces cannot be produced at economically acceptable costs; therefore, rough surfaces are often applied. This is especially true for large mechanical structures using polymer materials and steel counter-bodies. Generally, the formation of a polymer debris transfer film on intermediate rough steel surfaces can reduce abrasive actions caused by the asperities of the steel [3]. However, for very high roughness of the steel counter-body, the smoothening of asperities may be unachievable or may require a significant amount of operating time. At the same time, polymer wear particles cannot completely fill the valleys and the peaks of the steel surface over long periods of operation or even during the entire lifetime. The combination of these different phenomena strongly

affects the static friction of such pairings. Furthermore, the high load-carrying polymers such as polyamides (PA) are very sensitive to the environmental humidity due to their high polarity and their consequent high intake of water [8]. Therefore, these aspects should also be considered when using this type of material pairings in any industrial applications.

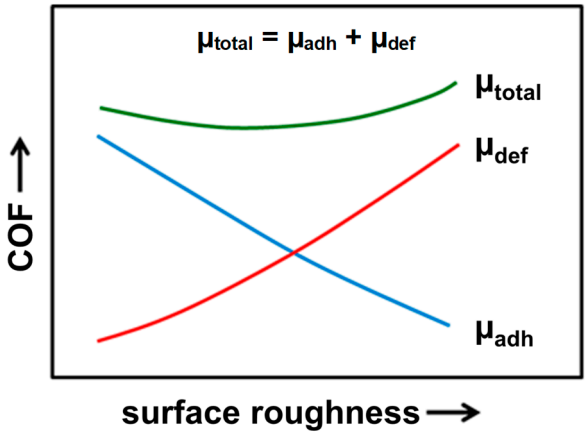


**Figure 1.** Influence of the surface roughness on the adhesive and deformative components of the coefficient of friction (COF or μ) (adapted from [9]).

For the presently investigated lubricated surfaces, adhesion effects caused by surface energy can be neglected, because deformation dominates the friction effects. In contrast to plastic-plastic contacts where the surface roughness has a minor significance on the friction behaviour, in plastic-metal contacts the surface roughness is essential for a good functionality [9].

For tribological contacts involving a soft polymer compressed against a metallic partner, the surface roughness asperities of the metallic counterpart penetrate into the polymer and this occurs without any deformation of the surface asperities of the metal itself. Under a simplified assumption of an elastic contact (neglecting any plastic deformation of the polymer), the penetration of a single roughness peak of the metallic counterpart into a smooth polymer surface can be described by a Hertz's equation [9]:

$$h \sim {F_N}^{1/3} \times (1 - \nu^2)^{2/3} \times E^{-2/3} \quad (1)$$

where $h$ is the penetration depth, $F_N$ the normal force, $\nu$ is the Poisson's ratio and $E$ is the modulus of elasticity. As already published elsewhere [10], the friction force ($F_R$) is a product of the shear strength $\tau_s$ of the materials and the real contact area ($A_r$) between both surfaces:

$$F_R \sim \tau_s \times A_r \quad (2)$$

By assuming the presence of a correlation between penetration depth ($h$ of Equation (1)) and measured compressive yield stress ($\sigma_{dF}$), the coefficient of friction resulting from rough surfaces may be described by the following equation [9]:

$$\mu = \tau_s / \sigma_{dF} \times 1/({F_N}^{1-n}) \quad (3)$$

The above equation may be used in order to describe the load dependency of the coefficient of friction for polymers on rough surfaces, wherein for polymers the exponent $n < 1$ [9].

## 2. Experimental

In the present study, two different PA6 polymers with and without solid lubricant inclusions were tested against a S1100QL steel surface having a very high surface roughness ($R_z \approx 40$ μm) or a normal roughness value ($R_z \approx 5$ μm). Table 1 lists some properties of both PA6 materials while Table 2 lists some properties of the steel plates used for the actual investigations. Values listed in Table 1 were

not measured but taken from manufacturer's data sheets and should be seen as nominal values only. Mechanical properties of the PA6-based polymers under study at 100% water content are not listed in this table but could be roughly extrapolated from a comparison of the values under dry and normal (50% relative humidity) conditions. Since properties at 50% humidity are deteriorated in comparison to properties under dry conditions, it is expected that mechanical properties of PA6 polymers at 100% water content will be more deteriorated than at 50% relative humidity.

**Table 1.** Selected properties of both PA6 polymers used for the tribological investigations. [1.]

| Property | Environmental Conditions | Value | |
|---|---|---|---|
| | | Pure PA6 | Friction-Modified PA6 |
| Tensile strength; N/mm$^2$ | dry conditions | 85 | 95 |
| | normal conditions [2] | 65 | 70 |
| Tearing strength; % | dry conditions | 50 | >25 |
| | normal conditions [2] | 120 | no data |
| Modulus of elasticity; N/mm$^2$ | dry conditions | 3700 | 3500 |
| | normal conditions [2] | 2800 | 2800 |
| Ball pressure hardness; N/mm$^2$ | dry conditions | 160 | 160 |
| | normal conditions [2] | 125 | 130 |
| Moisture absorption (23 °C/50%rh); % | — | 1.8 | 1 |

[1] Values given are nominal values determined by the manufacturer; [2] Normal conditions: 23°C/50%rh.

**Table 2.** Selected properties of steel plates used for the tribological investigations.

| Property | Value |
|---|---|
| Manufacturer/Product ID | S1100QL (1.8942) |
| Surface pre-treatment | Zn-based primer [1] |
| Surface roughness $R_z$ | 38 µm (roughened); 5 µm (grinded) |

[1] Two-component solvent-borne zinc ethyl silicate primer used for corrosion protection.

The pure PA6 material consisted of normal commercially available PA6. The friction-modified PA6 consisted of the same pure PA6 to which 6 wt % of solid lubricants (PTFE particles + oil) were added in order to enhance its frictional properties. It is worth noting again that both PA6 materials were commercially purchased and no further treatments (besides the change of their water contents) were performed on them by the authors, that is, the friction-modified PA6 was not developed by the authors and the actual process used for the addition of PTFE and oil to PA6 may not be divulgated in the present manuscript since this is proprietary to the manufacturer. Both PTFE and oil added to the friction-modified PA6 polymer act as lubricants in order to minimize the friction coefficient: oil addition is aimed for a fast-delivery lubricating action, while PTFE is responsible for long-duration lubricating effects.

As mentioned previously, the steel plates consisted of S1100QL, which is also denominated as 1.8942 steel. The choice of this steel was based on the fact that the actual study is part of an industrially financed research project, in which this steel was used as the main counter body in the tribological application. These plates were firstly surface treated using a Zn-based primer in order to enhance their corrosion resistance, as usually performed for the actual industrial application. Prior to this surface treatment, the blank steel surface was either roughened or grinded in order to obtain different surface roughness values. The roughening procedure enabled the production of very rough steel surfaces with roughness values of $R_z \approx 40$ µm, while through the grinding process, it was possible to obtain very smooth steel surface with roughness values of $R_z \approx 5$ µm. Surface roughness of investigated steel plates were measured using a commercially available non-contact 3D optical interferometer (µSurf, NanoFocus AG, Oberhausen, Germany). It is worth noting here that both represented topographies

of the steel plate correspond to extreme cases encountered in the actual industrial application: the roughened topography (rough steel surface) corresponds to the steel surface before its implementation in the application and the grinded pattern (smooth steel surface) corresponds to the steel surface after years of use. Therefore, both surface topographies were chosen in order to study any possible effect on their friction behaviour.

Prior to perform the tribological tests, PA6 samples of both types (pure and friction-modified) were conditioned in order to modify their water content, which actually also results in a change of their mechanical properties, as listed in Table 1. Several PA6 samples were put in a furnace at a temperature of 70 °C and 0%rh for several hours until their weight was stable, that is, until no weight change due to water loss could be measured. These dried samples are thereafter denominated as 0%-water saturated or dried samples. On the other hand, other PA6 samples were immersed in water at a temperature of 80 °C for a total duration of approximately 120 h. This previously optimized duration was determined by weighing the samples before the immersion process and at each hour of wetting until stable water saturation was reached. Depending on the PA6 material used (pure or friction-modified), the highest total water saturation was ranging between 5 wt % and 6.5 wt %, as shown in Figure 2. These wet samples are hereafter denominated as water saturated or wet samples.

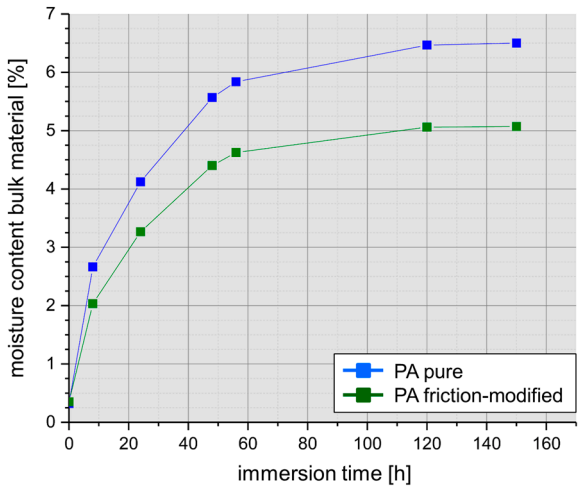


**Figure 2.** Measured moisture content of investigated pure and friction-modified PA6 polymers in function of water immersion time.

Both static and dynamic frictional test measurements were conducted on a universal modular designed tribometer (RVM1000, Werner Stehr Tribologie, Horb-Ahldorf, Germany), as shown in Figure 3a, using contact geometry as shown in Figure 3b. Figure 3c,d show a detailed view of the geometry of the PA6 samples used in these tribological tests and the actual shape of both lips in contact with the steel plate is rectangular and is schematically shown in Figure 3d. Each lip has dimensions of 1.5 × 7 mm resulting in a contact area of approximately 10.5 $mm^2$ for each lip and a total nominal contact area per polymer sample (for both lips) of 21 $mm^2$. The contact track of each lip does not interfere with the track of the other lip, in other words, the lip tracks do not overlap each other. Static and dynamic friction was analysed under a series of nominal contact pressures (from 40 $N/mm^2$ down to 2.5 $N/mm^2$), which were steadily decreased during the tests, as schematically shown in Figure 4. This procedure of reducing (instead of increasing) the nominal contact pressures during tribological testing was chosen in order to eliminate any additional plastic deformation variations (which may occur at high contact pressure values) during a measurement cycle. The influences of polymer water saturation, counter-body surface roughness, lubrication and temperature were also investigated, as listed in Table 3 which also lists the main testing parameters used for the tribological tests. It is worth noting that the time duration of each load step was chosen in order to have duration as long as possible in order to obtain stable and statistically significant friction values and on the other hand as short

as possible in order to minimize or eliminate any occurrence of wear mechanisms that could have significantly impaired or interfered with a correct friction analysis. Furthermore, due to the soft nature of PA6 samples in comparison to the primer-coated steel used, no wear or topographical changes of the steel may have occurred under the investigated testing conditions. Therefore, no wear investigations of PA6 or steel samples were performed in this study.

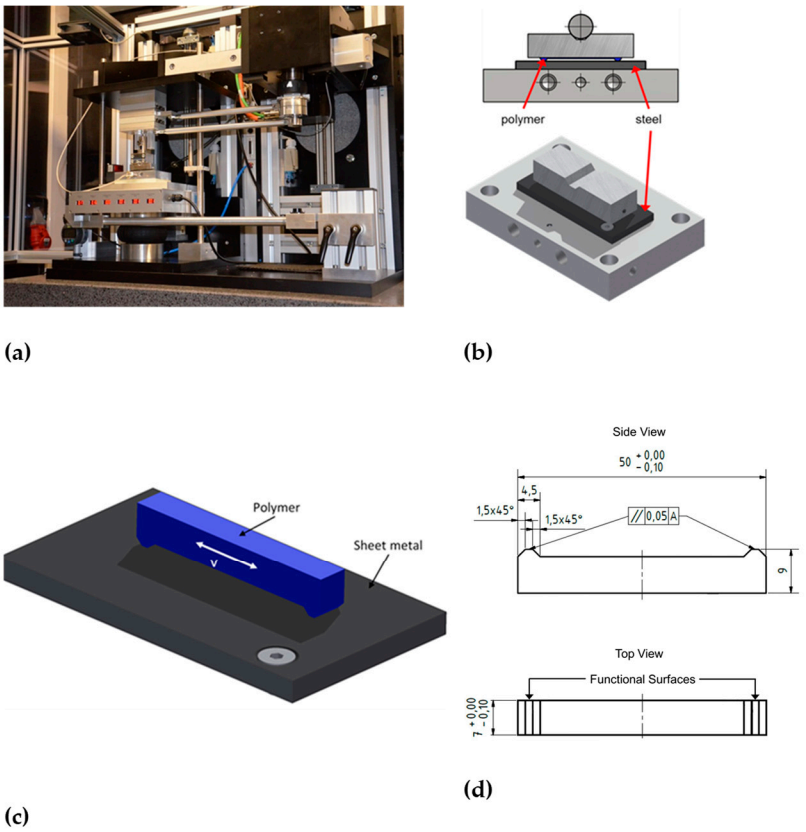


**Figure 3.** Test setup used for the tribological investigations: (**a**) modular designed tribometer, (**b**) close-ups of the testing geometry, (**c**) close-up of the tested samples geometry and (**d**) dimensions of the upper polymer sample.

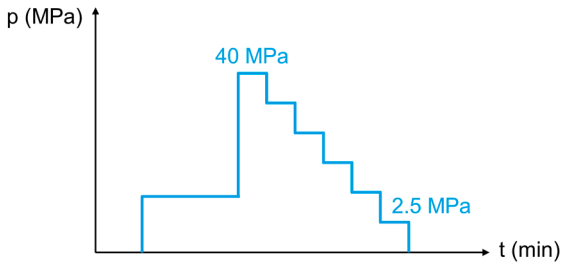


**Figure 4.** Schematic of the load-decreasing tribological tests performed to determine the static and dynamic friction coefficients of both PA6 polymers against steel plates (surface contact pressure $p$ in MPa as a function of time $t$ in minutes).

**Table 3.** Selected test parameters used for the tribological investigations.

| Property | Value |
|---|---|
| Nominal contact pressure | $2.5\ \mathrm{N/mm^2} \leq x \leq 40\ \mathrm{N/mm^2}$ |
| Nominal contact area | $\approx 21\ \mathrm{mm^2}$ |
| Sliding velocity (average) | 0.2 m/s |
| Stroke | 24 mm |
| Total test duration | 15 minutes |
| Temperature | 22 °C; 80 °C |
| Lubrication | grease lubricated (mineral oil, calcium complex soap, NLGI class 2); none (unlubricated: only for $R_z \approx 5$ µm) [1] |

[1] Unlubricated tribological investigations were conducted only against smooth steel plates ($R_z \approx 5$ µm), for which wear of pure and friction-modified PA6 materials in dry or wet conditions was relatively small.

The main analysis of the obtained raw friction data consisted of the determination of static and dynamic coefficients of friction. This was performed firstly by searching the initial peak in the friction values at the beginning of each cycle and at the turning point (end of stroke); both points corresponding to the onset of motion of the samples and these two static friction values are identified by arrows in Figure 5a. On the other hand, the dynamic friction coefficients were calculated by averaging the raw sliding friction values between both turning points for each cycle. In order to take into account only stable raw sliding friction values, a time window eliminating 10% of the values at the beginning and at the end of a half-cycle was used, as shown by the green zones in Figure 5a. That means that the sliding COF is an average value over a range of different velocities as they occur due to the sinusoidal movement. With this calculation, the influence of the sliding velocity on the COF is lost but as it can be observed in Figure 5a, there is only a minor influence of the sliding velocity on the COF within the used velocity regime. It is important to note that the diagram shown in Figure 5a shows only 1 complete linear reciprocating cycle of the corresponding tests at different contact pressures. It is also worth noting that the analysis of the raw signals was performed not only on 1 cycle but the COF values were averaged over all 5 strokes of each load step and within each load step, no specific trends in the measured COF values could be observed.

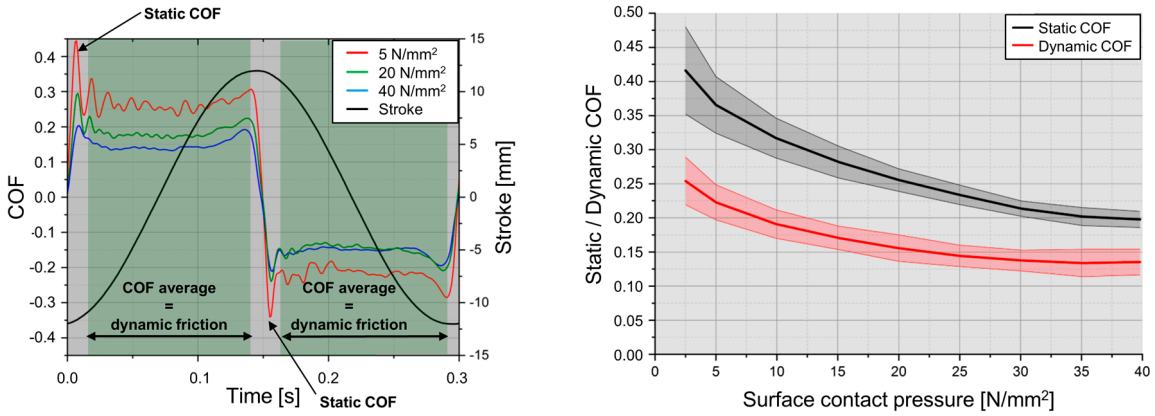


(**a**) (**b**)

**Figure 5.** (**a**) Diagram describing the analysis performed on raw friction results used for the determination of the static and dynamic friction coefficients (example shown: 1 complete linear reciprocating cycle for pure PA6 against rough steel with $R_z \approx 40$ µm at three different contact pressures: 5, 20 and 40 $\mathrm{N/mm^2}$) and (**b**) example of analysis results over the whole contact pressure range (example shown: pure PA6 against rough steel with $R_z \approx 40$ µm).

Figure 5b shows an example of the obtained values for the static (black) and dynamic (red) friction coefficients over the whole contact pressure range (2.5 $\mathrm{N/mm^2}$ to 40 $\mathrm{N/mm^2}$) under study. The middle solid lines represent the averages of at least two tests and the coloured regions around the averages

represent the variance of the obtained friction data. In the following sections, a certain number of diagrams do not show any coloured regions around the average curves: for these results, only one tribological test was conducted and therefore, no statistical analysis could be performed nor presented.

## 3. Results and Discussions

The aforementioned surface pre-treatment processes performed on the steel plates have a significant influence on their obtained surface roughness values, as shown in Figure 6. As expected, the roughening process produced the highest surface roughness values ($R_z \approx 40$ µm) while the grinding process induced the lowest surface roughness ($R_z \approx 5$ µm). Furthermore, through a detailed observation of the topographies, one may see that the surface roughness of the roughened samples (Figure 6a) possess a stochastic surface structure while samples processed through grinding (Figure 6b) possess a strongly oriented surface structure in the form of parallel lines. Both observed surface structures are well known in the literature and are typical for the processes used.

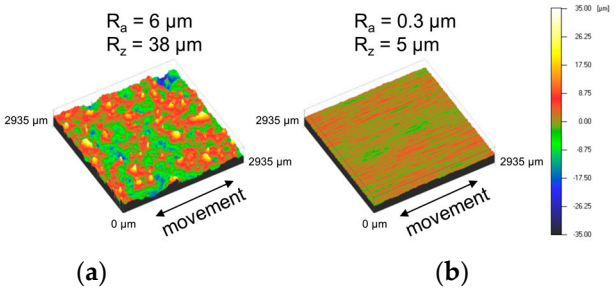


**Figure 6.** Typical topographies and measured surface roughness values of (**a**) roughened (rough surface: $R_z \approx 40$ µm) and (**b**) grinded (smooth surface: $R_z \approx 5$ µm) steel plates.

Figure 7 shows static friction coefficients and Figure 8 shows dynamic friction coefficients for both PA6 materials (pure and friction-modified) at both water saturation levels (0% and 100%) against a rough steel plate ($R_z \approx 40$ µm) under lubricated conditions at 22°C. First of all, as shown earlier by Equation (3), described elsewhere [9] and observed in Figures 7 and 8, a load dependency of the coefficient of friction may be observed for both static and dynamic frictions. Due to a nonlinear behaviour between friction force and normal load, the coefficient of friction decreases with increasing normal load [11].

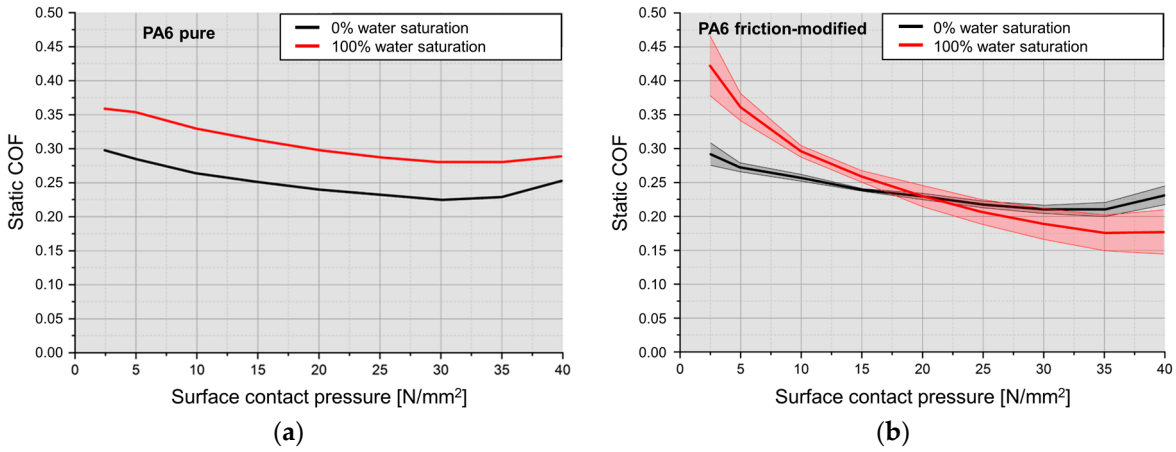


**Figure 7.** Static friction of investigated PA6 polymers against a lubricated rough steel plate ($R_z \approx 40$ µm) for both water saturation levels (0%, 100%) at 22°C: (**a**) pure PA6 and (**b**) friction-modified PA6.

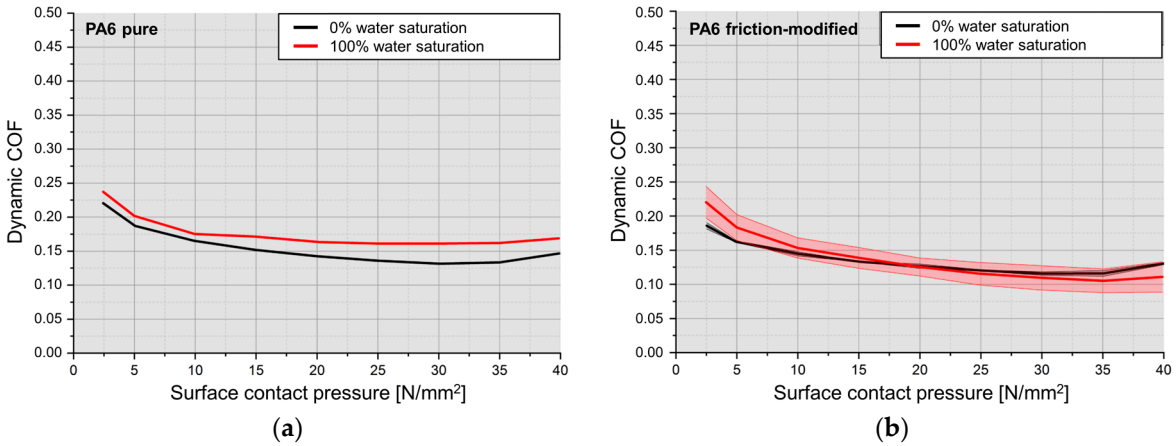


**Figure 8.** Dynamic friction of investigated PA6 against a lubricated rough steel plate ($R_z \approx 40$ µm) for both water saturation levels (0%, 100%) at 22°C: (**a**) pure PA6 and (**b**) friction-modified PA6.

For both investigated polymers at low normal loads, static friction coefficients were higher for wet (100% water saturation) than for dry (0% water saturation) samples, due to the softening of the polymer through higher water absorption and the consequent higher induced deformative friction (Figure 7). However, for friction-modified PA6 at high contact pressures (Figure 7b), this friction increase due to moisture was not observed anymore, since penetration depths of the steel plates into the highly moisturized PA6 polymer reach a saturation state and therefore the compressive yield stress of the polymers determines mostly the friction behaviour.

Again for both investigated polymers, dynamic friction coefficients were approximately similar for wet (100% water saturation) and for dry (0% water saturation) samples. A detailed explanation of these behaviours resides in the fact that a low moisture content in PA6 polymers leads to a higher *E*-modulus and compressive yield stress, resulting in a lower penetration depth when using the previously presented Equations (1) and (3) and therefore at low loads, providing a lower coefficient of friction. For PA6 polymers with higher moisture content, the contrary occurs: a lower *E*-modulus and compressive yield stress results at low loads in a higher coefficient of friction. Although at high loads, roughness asperities penetrate deeper into the polymer with the higher moisture content, the resulting shear forces are lower. On the other hand for the material with the low moisture content, the shear forces grow disproportionately with increasing loads, whereby the coefficient of friction for the low moisture content material at high load is higher than with the lower moisture content.

By comparing curves shown in Figures 7 and 8 (Figs. a versus Figs. b), it may be observed that at 0% water saturation (black curves), both static and dynamic friction coefficients of both PA6 materials (pure and friction-modified) are almost similar but for 100% water saturation, both materials possess quite different friction behaviours. The overall behaviours of both polymers may be observed in Figure 9, which shows the difference between both static and dynamic frictions: a higher stick-slip tendency [12] may be observed at low normal loads for both PA6 materials at the higher water content (100% water saturation). Overall, the experimental investigations involving both PA6 polymers against rough surfaces ($R_z \approx 40$ µm) have shown that depending on the moisture content of the PA6 polymers, their mechanical properties are determinant for the static friction force values. It is worth noting that the results obtained and presented in Figures 7–9 from the tribological tests performed against a rough steel surface ($R_z \approx 40$ µm) are difficult to compare with previously published results from the scientific community because such rough surfaces are usually not the focus of tribological investigations.

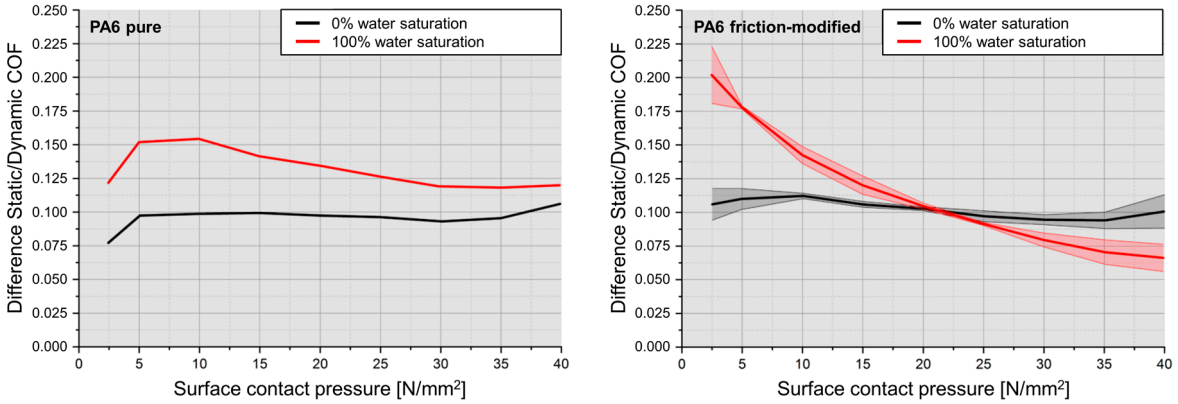


**Figure 9.** Difference between static and dynamic frictions of investigated PA6 polymers against a lubricated rough steel plate ($R_z \approx 40$ µm) for both water saturations (0%, 100%) at 22°C: (**a**) pure PA6 and (**b**) friction-modified PA6.

Results obtained from investigations of both PA6 materials (pure and friction-modified) at both water saturation levels (0% and 100%) against a smooth steel plate ($R_z \approx 5$ µm) under lubricated and unlubricated conditions at 22 °C are shown in Figure 10 (static friction coefficients) and in Figure 11 (dynamic friction coefficients). It is worth noting here that unlubricated tribological tests were conducted only for both PA6 materials against smooth steel plates ($R_z \approx 5$ µm), for which it was observed that their wear in both dry and wet conditions was minimal and thus, any influence of occurring wear mechanism could be discarded from the analysis of the friction behaviour.

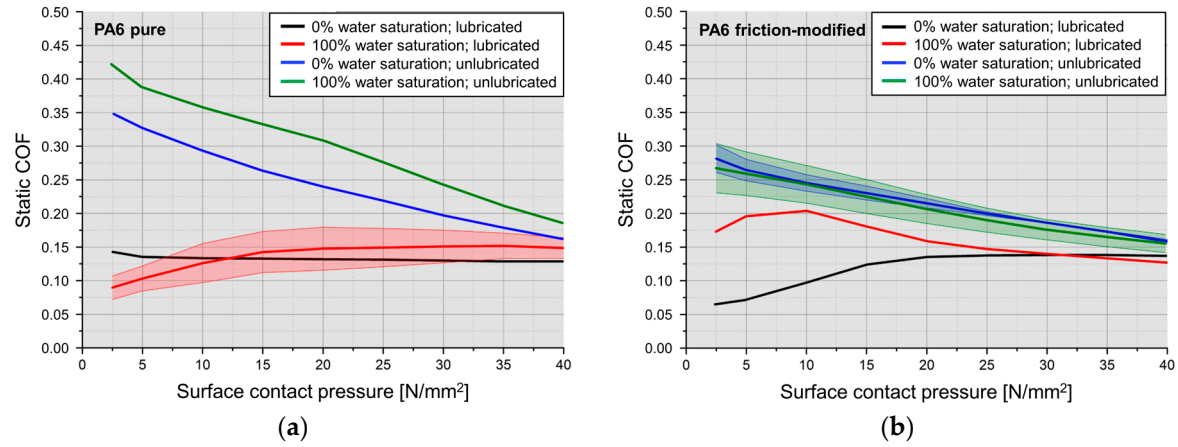


**Figure 10.** Static friction of investigated PA6 polymers against a lubricated and unlubricated smooth steel plate ($R_z \approx 5$ µm) for both water saturation levels (0%, 100%) at 22°C: (**a**) pure PA6 and (**b**) friction-modified PA6.

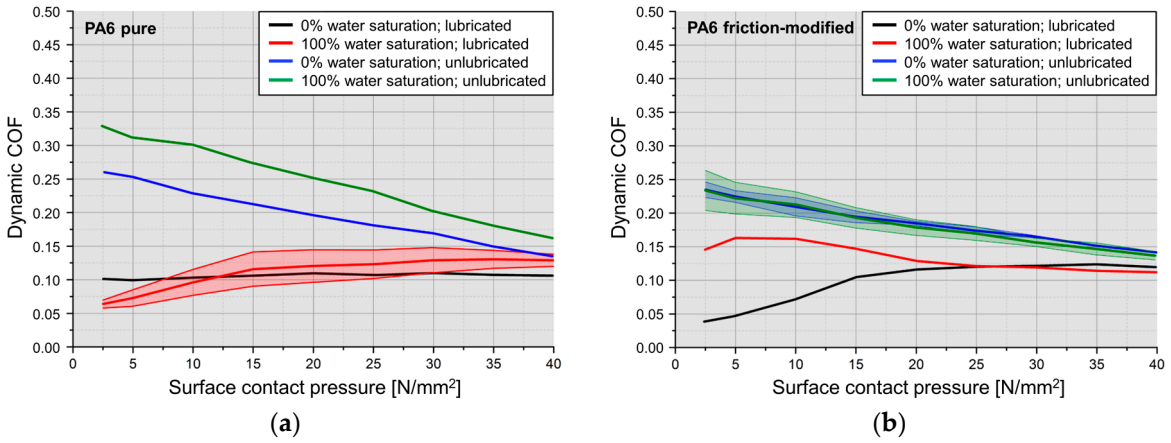


**Figure 11.** Dynamic friction of investigated PA6 polymers against a lubricated and unlubricated smooth steel plate ($R_z \approx 5$ µm) for both water saturation levels (0%, 100%) at 22 °C: (**a**) pure PA6 and (**b**) friction-modified PA6.

A comparison of results for the lubricated conditions presented in Figures 10–12 with previous results presented in Figures 7–9 shows that a reduction of the surface roughness (from $R_z \approx 40$ µm to $R_z \approx 5$ µm) leads to a reduction of the coefficient of friction, which is mostly due to a decrease of the penetration depth of the steel surface into the polymers: the deformative part of friction is drastically reduced and the adhesive part of friction is also negligible, due to the lubricated conditions used during the tribological tests.

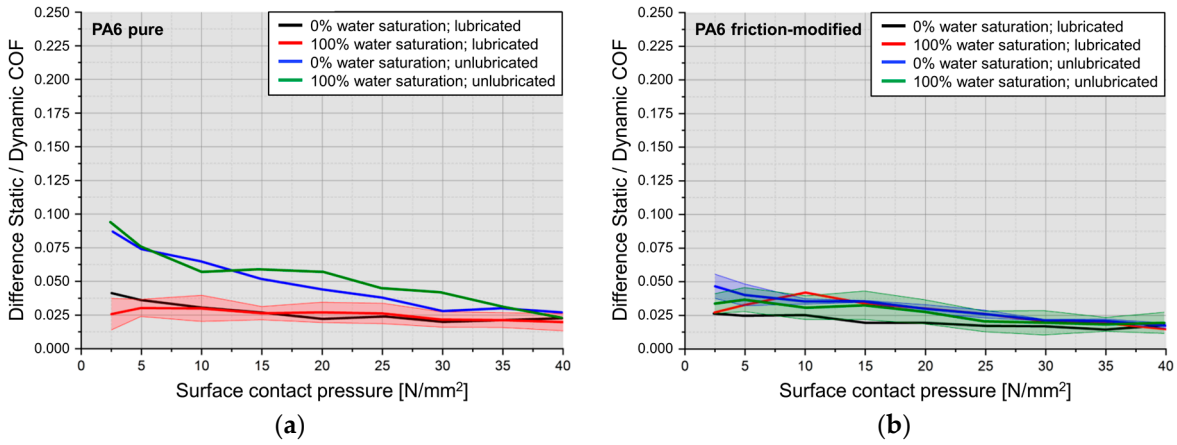


**Figure 12.** Difference between static and dynamic frictions of investigated PA6 polymers against a lubricated or unlubricated smooth steel plate ($R_z \approx 5$ µm) for both water saturations (0%, 100%) at 22 °C: (**a**) pure PA6 and (**b**) friction-modified PA6.

On the other hand, when comparing the same results for the dry samples under unlubricated conditions (Figures 10–12 with Figures 7–9), a reduction of the surface roughness (from $R_z \approx 40$ µm to $R_z \approx 5$ µm) leads to a significant increase of the coefficient of friction, which is due to the fact that PA6 is highly polar and under predominantly adhesive sliding conditions (smooth steel surfaces, low contact pressure values and no lubrication), the adhesive frictional part plays a dominant role in the overall friction, as also reported elsewhere [6,7,13].

Results obtained for both PA6-based materials investigated in the present study are quite comparable with previously published work in which the testing parameters were different than those of the present study. Sliding coefficients of friction of 0.3 to 0.4 were reported for PA6.6 against 100Cr6-steel with a $R_z \approx 3$ µm under dry unlubricated conditions at a velocity of 0.5 mm/s and at room temperature for contact pressures of 1 MPa and 8 MPa respectively [13]; results which are slightly

higher than the values presented in Figure 11a (blue curve for PA6, 0% humidity, unlubricated: $\mu \approx$ 0.28 at 2.5 MPa and $\mu \approx 0.23$ at 8 MPa). In another study [7], static coefficients of friction ranging between 0.35 and 0.50 and sliding coefficients of friction ranging between 0.25 and 0.35 were reported for PA6 and PA6.6 against carbon steel (S235JR) with a $R_z \approx 5$ µm under dry unlubricated conditions at a velocity of 10 mm/s and at room temperature for a contact pressure of 10 MPa. These results are quite comparable with the values presented in Figure 10a (blue curve for PA6, 0% humidity, unlubricated: static $\mu \approx 0.30$ at 10 MPa) and Figure 11a (blue curve for PA6, 0% humidity, unlubricated: sliding $\mu \approx 0.23$ at 10 MPa). The small discrepancies between the results of the present study and results from both mentioned previously published works are believed to be due to the differences in the testing parameters used, especially the test velocity.

By comparing results from pure PA6 to results from friction-modified PA6 shown in Figures 10–12, one may observe that for medium and high surface contact pressure values, both PA6 materials possess similar friction coefficients (static, dynamic and difference between both of them) independently of the other varied tests conditions (water saturation or lubrication status of the tribological contact). These results show that, at these medium and high contact pressure values, the mechanical properties of PA6 polymers have only a minor influence on their overall friction behaviour. On the other hand, for low surface pressures, some differences between both PA6 materials may be easily observed. Firstly, for unlubricated contacts at 0% water saturation, slight differences could be identified between both PA6 materials. For unlubricated conditions at 100% water saturation, friction-modified PA6 exhibits slightly lower stiction and dynamic friction coefficients than pure PA6, showing that the latter possess a higher tendency for stick-slip. For lubricated contacts at 0% water saturation, static and dynamic friction coefficients of pure PA6 are lightly higher than those of friction-modified PA6 and at 100% water saturation, an opposite behaviour may be observed: static and dynamic friction coefficients of pure PA6 are lightly lower than the values obtained for friction-modified PA6. A comparison of the diagrams shown in Figure 12 (difference between static and dynamic frictions) shows clearly that for PA6 against a smooth steel surface ($R_z \approx 5$ µm) under lubricated conditions, both PA6 polymers shows similar trends and approximately equivalent values independently of the water content and that under unlubricated conditions, pure PA6 tends to have a higher tendency to stick-slip than friction-modified PA6. These behaviours are due to the fact that against a smooth steel surface, the deformative part of friction is significantly reduced through a lower indentation of the steel surface into the polymer. Furthermore, for the friction-modified PA6, the enhanced mechanical properties contribute to a further reduction of the deformative friction. Additionally, to these reductions of the deformative friction for both PA6 polymers, a supplementary reduction of the adhesive friction is achieved through the lubricated conditions, rendering a significant decrease of the overall friction coefficients.

To perform a more detailed analysis of the obtained results, the effect of the water saturation level of both PA6 materials under study may be analysed by comparing the results shown in Figures 10–12. For pure PA6 under lubricated conditions, static (Figure 10a), dynamic (Figure 11a) and resulting difference between both friction coefficients (Figure 12a) are approximately similar between wet samples (100% water saturation) and dry samples (0% water saturation), while under unlubricated conditions, static and dynamic friction coefficients are higher for the wet samples but the difference between both coefficients are similar. These behaviours are again mainly due to the relationship between indentation depth of steel and softening of the pure PA6 at high water content levels. For friction-modified PA6 under lubricated conditions, static (Figure 10b) and dynamic (Figure 11b) friction coefficients are higher for the wet samples at low loads only but the difference between both coefficients (Figure 12b) is similar, while under unlubricated conditions, static, dynamic and difference between both friction coefficients are approximately similar between wet samples (100% water saturation) and dry samples (0% water saturation). Again, these behaviours are mainly due to the relationship between indentation depth of steel and to the enhanced mechanical properties of the friction-modified PA6. Furthermore, results shown in Figure 12 deliver a more obvious confirmation that the water saturation

level does not have an important influence on the overall friction behaviour of both PA6 materials under study.

To perform a more detailed analysis of the obtained results, the influence of the use of lubrication in the tribological contact may be analysed by comparing results shown in Figures 10–12. In these diagrams, it may be observed that tests performed under lubricated conditions at a specific water saturation level deliver similar friction behaviours for pure PA6 but small divergences are observed for the friction-modified PA6 at low surface contact pressure values. On the other hand, for tests performed under unlubricated conditions, different friction behaviours are observed. For the friction-modified PA6, both static (Figure 10b) and dynamic (Figure 11b) frictions are, independently from the water saturation level, slightly higher for the unlubricated than for the lubricated conditions but the overall difference between static and dynamic frictions (Figure 12b) stays approximately equivalent. For the pure PA6, a significant increase of static (Figure 10a), dynamic (Figure 11a) as well as the difference between both frictions coefficients (Figure 12a), independently from the water saturation level, may be observed when performing the tests under unlubricated conditions in comparison to lubricated ones. This behaviour is due to the well-known ability of lubricants to lower the adhesive part of friction.

Figure 13 shows the influence of the test temperature (22 °C or 80 °C) on both coefficients of friction (Figure 13a: static; Figure 13b: dynamic) of both PA6 polymers in both investigated water saturation levels (0% and 100%) against a rough steel plate ($R_z \approx 40$ µm) under lubricated conditions. It is worth noting here that the results of the influence of temperature are only presented for tests performed against a rough steel plate ($R_z \approx 40$ µm), since the major differences were observed for this surface roughness value and also in order to keep the actual manuscript as short and concise as possible but similar results were obtained and similar conclusions as those presented for tests performed against a rough steel plate may be drawn for both polymers against a smooth steel plate ($R_z \approx 5$ µm).

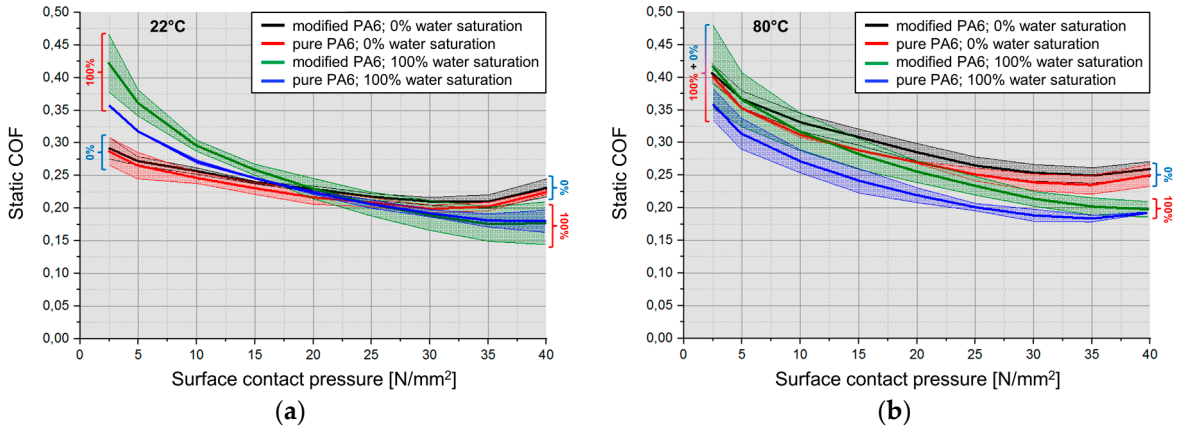


**Figure 13.** Static friction coefficients of investigated PA6 polymers against a lubricated rough steel plate ($R_z \approx 40$ µm) for both water saturation levels (0%, 100%) at: (**a**) 22 °C and (**b**) 80 °C.

From Figure 13, it may be observed that static friction coefficients for both PA6 materials for both water saturation levels (0% and 100%) at 80 °C (Figure 13b) are slightly higher than the results obtained at 22 °C (Figure 13a). Generally, when polymers are heated, a decrease in their mechanical properties is normally induced (lower *E*-modulus and compressive yield stress), which results in a deeper penetration depth of the asperities of the steel counterpart; the penetration depth is even more important when the surface roughness of the steel plate is high and the combination of these effects result in a slightly higher coefficient of friction at high temperature.

Finally, the experimental investigations involving both PA6 polymers against a rough surface ($R_z \approx 40$ µm) under lubricated conditions have shown that depending on their moisture contents and

on their temperatures, the mechanical properties of the polymers are actually the determining factor which governs their static friction forces.

## 4. Conclusions

For the investigated polymer-steel tribological systems that have different surface roughness values under different environmental conditions of water saturation and temperature presented in the actual study, the following main conclusions may be drawn:

1. The surface roughness of the steel counterpart plays a significant role in the overall friction behaviour of the studied tribological systems: (a) The rougher the steel surface, the more determinant the deformative component of friction. (b) The smoother the steel surface, the more determinant the adhesive component of friction.
2. The relationship between the penetration depth of the steel surface into the polymer material, the compressive yield stress of the polymer itself and the normal load mainly determines the friction behaviour: (a) For low loads, reduced mechanical properties of the PA6 polymers lead to higher penetration depths. (b) For high loads, penetration depths into the PA6 polymers (even with different mechanical properties) reach a saturation state and therefore, the compressive yield stress of the PA6 polymers mostly determines their friction behaviours. (c) Independently of the method used to reduce the mechanical properties of the PA6 polymers (either through a variation of moisture content or temperature), the resulting friction behaviours are always comparable under the actual investigated test conditions. (d) Contrary to many previously published assumptions, mechanical properties of polymers have only a minor influence on their friction behaviours at high loads.

It is here important to highlight that the aforementioned observations and conclusions are drawn solely for the friction behaviour and not for the wear behaviour of the investigated tribological systems.

**Author Contributions:** Conceptualization, S.K. and A.D.; Data curation, S.K.; Formal analysis, S.K. and A.D.; Funding acquisition, A.D.; Investigation, J.V., S.K. and F.A.; Methodology, J.V., S.K. and A.D.; Project administration, S.K. and A.D.; Resources, S.K. and F.A.; Supervision, A.D.; Validation, J.V., S.K. and A.D.; Visualization, J.V., S.K., I.V., F.A. and A.D.; Writing—original draft, J.V., S.K., I.V. and F.A.; Writing—review & editing, J.V., S.K., I.V. and A.D.

**Funding:** This research was partially funded by the Austrian COMET Programme (Project XTribology), grant number 849109 and carried out at the "Excellence Centre of Tribology" (AC$^2$T research GmbH) in cooperation with V-Research GmbH.

**Conflicts of Interest:** The authors declare no conflict of interest. The founding sponsors had no role in the design of the study; in the collection, analyses or interpretation of data; in the writing of the manuscript and in the decision to publish the results.

## References

1. Sinha, S.K. *Handbook of Polymer Tribology*; World Scientific Publishing: Singapore, 2018; ISBN 978-9-81322-778-1.
2. Myshkin, N.K.; Pesetskii, S.S.; Grigoriev, A.Ya. Polymer Tribology—Current State and Applications. *Tribo. Ind.* **2015**, *37*, 284–290.
3. Myshkin, N.K.; Petrokovets, M.I.; Kovalev, A.V. Tribology of polymers: Adhesion, friction, wear and mass-transfer. *Tribol. Int.* **2005**, *38*, 910–921. [CrossRef]
4. Pesetskii, S.S.; Bogdanovich, S.P. Polymer composites and nanocomposites. In *Encyclopedia of Tribology*; Wang, Q., Chung, Y.-W., Eds.; Springer: New York, NY, USA, 2013; pp. 2563–2570.
5. Li, D.; Xie, Y.; Li, W.; You, Y.; Deng, X. Tribological and Mechanical Behaviors of Polyamide 6/Glass Fiber Composite Filled with Various Solid Lubricants. *Sci. World J.* **2013**, *2013*, 320837. [CrossRef] [PubMed]
6. Quaglini, V.; Dubini, P.; Ferroni, D.; Poggi, C. Influence of counterface roughness on friction properties of engineering plastics for bearing applications. *Mater. Des.* **2009**, *30*, 1650–1658. [CrossRef]

7. Rodriguez, V.; Sukumaran, J.; De Baets, P.; Ost, W.; Perez Delgado, Y.; Ando, M. Friction and wear properties of polyamides filled with molybdenum disulphide. *Mech. Eng. Lett. Res. Dev.* **2011**, *5*, 68–80.
8. Lancaster, J.K. A review of the influence of environmental humidity and water on friction, lubrication and wear. *Tribol. Int.* **1990**, *23*, 371–389. [CrossRef]
9. Erhart, G. Friction and wear behaviour of polymer materials (in German: Zum Reibungs- und Verschleißverhalten von Polymerwerkstoffen). Ph.D. Thesis, TH Karlsruhe University, Karlsruhe, Germany, 1980.
10. Bowden, F.P.; Tabor, D. *The Friction and Lubrication of Solids*, 2nd ed.; Clarendon Press: Oxford, UK, 1954; ISBN 0-19851-238-4.
11. Sinha, S.K.; Briscoe, B.J. *Polymer Tribology*; Imperial College Press: London, UK, 2009; ISBN 1-84816-202-2.
12. Popov, V.L. *Contact Mechanics and Friction (in German: Kontaktmechanik und Reibung)*; Springer: Berlin, Germany, 2009; ISBN 978-3-540-88836-9.
13. Erhard, G. *Designing with Plastics*; Carl Hanser Verlag: Munich, Germany, 2006; ISBN 978-3-540-88836-9.